Breath Rate Monitoring During Sleep using Near-IR Imagery and PCA

Manuel Martinez and Rainer Stiefelhagen
Institute of Anthropomatics, Karlsruhe Institute of Technology, Karlsruhe, Germany
manuel.martinez@kit.edu, rainer.stiefelhagen@kit.edu

Abstract

We present a vision based method to estimate the respiration rate of subjects from their chest movements. In contrast to alternative approaches, our method is fully automated, non-invasive, robust to occlusions, and only depends on off-the-shelf hardware. We project a fixed infrared (IR) dot pattern. The dots are detected using a camera with a matching IR filter. We estimate the dots' barycenters with sub-pixel precision and we track them over a 30 seconds sliding window. We merge all trajectories using Principal Component Analysis(PCA) and use Autoregressive (AR) Spectral Analysis to estimate the respiratory rate. The system was evaluated on 9 subjects and on a range of simulated scenarios using an artificial chest.

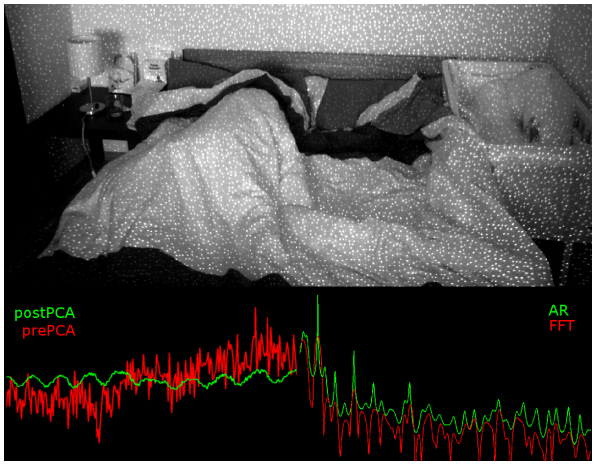

Figure 1. RR estimation on a 30s window, PCA filtered signal & AR power spectrum

1. Introduction and related work

Alterations of the respiratory rate (RR) are important markers of serious illness, and therefore RR is one of the main vital signs measured when performing clinical evaluations. Usually RR is measured by nursing staff by counting the number of chest excursions during a period of 30 seconds. A spirometer is used in cases where continuous monitoring is preferred. It directly measures airflow with a sensor, which can be a nasal cannulae, a mouthpiece, or a facemask.

Although these methods are convenient in hospital wards, for domestic or long term RR monitoring non-contact methods are preferred. There is a particular interest in RR monitoring during sleep, *e.g.* elderly care [2], prediction of risk events [1], and newborn monitoring [6, 12]. This problem has been studied from multiple fields but a practical system is still missing (see [1, 7]).

A general domestic monitoring system must be robust, autonomous, able to work without the collaboration of the monitored subject, easily installable on any domestic environment, and last but not least economic. Price rules out approaches that measure temperature changes associated to the breathing cycle [1, 6, 16] as they require thermal cameras. Skin color based methods [9, 14] estimate blood oxygen saturation to get the heart and breathing rates, but they can not work in the dark.

Several methods measure chest and abdominal movements, which has the advantage of being robust to occlusion. Doppler effect measurement has been studied using radar [5] and laser [12]. Computer Vision systems have found however limited success [8, 15]. But recent research using RGB-D, sensors such as Microsoft Kinect and ASUS Wavi Xtion, is promising [4].

The main limitation of those systems is the small movement typically evoked by respiration, which is around 10mm [13]. To overcome this limitation, passive systems require the subject to wear as much texture as possible [15], and stereoscopical systems use large baselines [2] or just close detection distances [4].

Our approach builds on the ideas brought by these systems. We use a Kinect which has been modified to project big IR dots. Each dot is tracked over 30 seconds and all trajectories are fused together using Principal Components Analysis. Finally, we perform an Autoregressive Spectral Analysis to obtain RR. Our method is designed to maximize the information extracted from the source images while still being a realtime approach. This allows us to estimate very small movements such as the ones induced by a sleeping person from a distance of 3 meters (see Fig. 1), where the mean amplitude of the movement is less than 0.048 pixels, or 0.0022 degrees.

We evaluated our breath rate estimator on 9 healthy subjects and compared our results with those of an inductance plethysmograph (RR measuring belt). Using an artificial system that simulates chest movements, we evaluated the distance and frequency limits of our system and compared them to those of an state-of-the-art alternative [4].

2. Estimating respiratory rate

2.1. Image sensor and camera model

Our system requires an IR dot pattern projector and a camera with a matching IR filter. For convenience we use a modified Kinect as it includes both devices.

The main goal of modifying Kinect was to improve the individual detection of the dots projected by the IR laser. We configured the IR camera to 1280x1024 pixels at 9.1 frames per second, and added a Niko Zoom lens only to the IR projector to increase the size of the dots. We detect an average of 15000 dots in the camera view.

Several parameters that must be taken into account in order to design the system. From the camera's point of view, when an object in the scene moves, the dots that are projected on it are displaced along the epipolar line. Using the pinhole camera model and the standard model for parallel cameras, the epipolar lines are $y = const$, and therefore the dots move only along the horizontal dimension.

The displacement magnitude depends on the focal length of the camera f; distance between camera and projector, or baseline b; magnitude of the object displacement d; distance to the object z; and angle of the displacement respect the angle of the camera α. Then Δx is the observed horizontal displacement of a dot in the image plane in pixels:

$$\Delta x = fb(\frac{1}{z} - \frac{1}{z'}) \qquad z' = z + d\ \cos(\alpha)\ , \quad (1)$$

$$\Delta x = \frac{f\ b}{z^2}\ \frac{d\ \cos(\alpha)}{1 + d/z\ \cos(\alpha)}\ , \quad (2)$$

then, if we assume $z \gg d$ we get:

$$\Delta x = \frac{f\ b}{z^2}\ d\ \cos(\alpha)\ . \quad (3)$$

We approximate f by using the rectilinear lens model from the horizontal resolution r and the angular field of view β:

$$f = \frac{r}{2\ \tan(\beta/2)}\ , \quad (4)$$

applying it to Eqn. 2 we get:

$$\Delta x = \frac{r\ b}{2\ z^2\ \tan(\beta/2)}\ d\ \cos(\alpha)\ . \quad (5)$$

Consequently, the pixel displacement can be improved by using a better resolution, larger baseline [2], smaller field of view or smaller distance to the object [4].

The Kinect camera has $\beta = 57.8°$ and $b = 75mm$. With the Kinect tilted $30°$ from the horizontal and pointing towards a person sleeping in supine position, a 10mm breathing amplitude translates to 1.74 pixels at $.5$ meters, 0.435 pixels at 1 meter, 0.109 pixels at 2 meters, and 0.027 pixels at 4 meters.

2.2. Estimating dot trajectories

We create tracks for every dot containing its trajectory over the last 30 seconds. First we highlight the dots on the current image by convoluting it with a 2D LoG kernel of matching size, in our case 9x9 pixels. We then find the local maximum for each dot with sub-pixel precision by computing the Center of Gravity [3] over a 5x5 pixel window. The tracking is performed frame by frame using a 3x3 pixel search window.

2.3. Feature Fusion using PCA

Image based algorithms usually produce a high number of features, often one per pixel, therefore complex fusion algorithms are commonly avoided and features are simply averaged (*e.g.*, [2, 4, 8, 14, 15]). In our case, we use the dot trajectories as features, and we only take into account dots with a complete 30s record. This reduces the typical amount of features to thousands instead of millions, and allows us to fuse the dots with a more elaborate method.

We experimentally found that the two major noise sources in our system are thermal noise, and mechanical vibration. The first noise shows no correlation between dots, but the second displays a strong correlation

between them. However, both types of noise are uncorrelated to the RR signal. In this scenario we can use Principal Component Analysis (PCA) to separate the signal component from the mechanical vibration, while reducing the level of thermal noise at the same time.

The principal components are calculated from a matrix containing the trajectories of each dot. We only need to calculate the first few components as we expect the RR signal and the correlated noise to be represented in the bases with most variance, and the thermal noise to be distributed between the remaining ones. We use the iterative EM [10] algorithm to efficiently calculate the 16 strongest components.

Then we discard noisy bases by using the Durbin-Watson test, as has been suggested by Ryu *et al.* [11]:

$$d_{\text{DW}} = \frac{\sum_{t=1}^{T}(v_t - v_{t-1})^2}{\sum_{t=0}^{T} v_t^2} \ , \tag{6}$$

d_{DW} lies between 0 and 4, and small values indicate a positive autocorrelation. All bases with d_{DW} above average are discarded. Then we obtain the Power Spectral Density (PSD) of the remaining bases using FFT, and discard the bases whose average power in the interest region (from 3 to 60 breaths per minute) is less than the average power outside the interest region.

Using the remaining bases we calculate an average trajectory with less noise, see Fig. 1.

2.4. Estimating RR from AR Spectral Analysis

Model based methods such as Autoregressive (AR) Spectral Analysis are often used in hearth and breath rate monitoring (*e.g.* [14]). An AR model can be seen as an Infinite Impulse Response filter that outputs an estimation of the data when it is excited by white noise. A pth order AR model is defined by:

$$X_t = \sum_{k=1}^{p} \varphi_k X_{k-i} + \varepsilon_t \ . \tag{7}$$

Once we estimate φ_k using Burg's maximum entropy method, we get the PSD of the process with:

$$S(f) = \frac{\sigma_{\text{Z}}^2}{|1 - \sum_{k=1}^{p} \varphi_k e^{-2\pi i k f}|^2} \ . \tag{8}$$

Where σ_{Z}^2 is the noise variance. The PSD obtained from the AR model presents narrower maxima than the PSD obtained from FFT, see Fig. 1. p id usually chosen empirically for each task, as higher order AR models contain more information and offer more precision, but are prone to split the main peak in two or more smaller peaks. We chose $p = 80$ based in our preliminary experiments.

The breathing rate is determined by scanning the PSD for local maximums inside the interest region. The frequency of each detected maximum is refined using the bisection method the strongest one is chosen.

3. Evaluation

3.1. Comparison to a plethysmograph

Our system was used to measure the breathing rate of 9 healthy subjects. They were asked to rest in our test bed, and then we monitored their breathing for two minutes from a distance of 1.5 meters to the chest and an angle of $45°$.

As the respiratory rate is a weakly defined measure, *e.g.*neither the minimum airflow nor the length of the measuring window are clearly regulated, we compared the results with those of an inductance plethysmograph: a MedTex180 based RR measuring belt. We obtained a correlation value of 0.995, and the null hypothesis of no correlation can be rejected with a *p-value* of 2.91^{-8}.

3.2. Range of operation

Using an artificial chest, we evaluated the range of operation of our system and compared it to that of an state-of-the-art alternative [4].

The artificial chest presents a surface of 30x20cm that simulates a respiration induced movement with the inhalation, exalation and pause periods with a movement amplitude of 10mm. In all tests it was covered by a white textureless bed sheet.

We chose Burba *et al.* [4], as a baseline system because it uses the same sensing device. Inhalation and exhalation periods are labeled by analyzing depth-averages over a 12 frame sliding window, then the elapsed time between consecutive breaths is used to estimate RR.

Range depends on the sensitivity of the system. We measured the capacity of each algorithm to discern the correct breath frequency over its harmonics and the background noise. We tested several RR and z combinations, 20 times per bin. A test was deemed successful when the algorithm provided an estimation within $\pm 10\%$ of the generated RR, and a failure otherwise. Success rate can be seen in Table 1. For our system we set up a Kinect 1m over the bed and aimed to the artificial chest. However, the Kinect was lowered to 50cm for our baseline system as we found necessary to test smaller z values.

ours	200 cm	300 cm	400 cm	500 cm
4 bpm	70	30	40	40
5.7 bpm	100	90	90	35
8.1 bpm	90	90	100	0
11.6 bpm	95	100	55	5
16.6 bpm	100	80	50	0
23.8 bpm	95	60	55	0
34.2 bpm	100	80	25	0
49.2 bpm	95	35	30	5

baseline	70 cm	85 cm	100 cm	115cm
4 bpm	0	0	0	0
5.7 bpm	0	50	10	0
8.1 bpm	25	85	45	5
11.6 bpm	65	60	05	0
16.6 bpm	45	25	10	0
23.8 bpm	20	15	10	0
34.2 bpm	5	15	0	0
49.2 bpm	0	10	15	0

Table 1. RR estimation success rate: Breaths Per Minute and Distance to the sensor (in %)

4. Conclusions and Future Work

We presented a vision based method to estimate the respiratory rate of sleeping subjects. Our system uses a modified Kinect to project dots and with its IR camera tracks the dots over 30 seconds. Trajectories are then filtered using a PCA based method and the respiratory rate is estimated using autoregresive spectral analysis. As our approach is non-invasive, autonomous, and depends only on affordable hardware, it facilitates the monitoring of patients in their own homes.

We have shown how to adapt this system to a custom environment, and we evaluated our test system in real as well as in simulated scenarios. Our results show that our approach provides good accuracy over a wider range of operating conditions than a similar approach using the same hardware.

However, our algorithm is only reliable when the subject is resting, and it can easily be fooled by sleep movements. Our next goal is to address this problem, common to all approaches that depend on chest movements.

Furthermore we want to extend our system by recognizing anomalous breathing patterns such as Cheyne-Stokes respiration or apnea, which can be simulated using our artificial chest. And we are also working on recognizing automatically multiple persons such as, *e.g.*couples.

References

[1] F. AL-Khalidi, R. Saatchi, D. Burke, H. Elphick, and S. Tan. Respiration rate monitoring methods: A review. *Pediatric Pulmonology*, 46(6):523–529, 2011.

[2] H. Aoki, Y. Takemura, K. Mimura, and M. Nakajima. Development of non-restrictive sensing system for sleeping person using fiber grating vision sensor. In *Micromechatronics and Human Science*, 2001.

[3] D. Bailey. Sub-pixel profiling. In *Information, Communications and Signal Processing*, 2005.

[4] N. Burba, M. Bolas, D. M. Krum, and E. A. Suma. Unobtrusive measurement of subtle nonverbal behaviors with the microsoft kinect. In *International Workshop on Ambient Information Technologies*, 2012.

[5] J. Geisheimer and I. Greneker, E.F. A non-contact lie detector using radar vital signs monitor (rvsm) technology. *Aerospace and Electronic Systems Magazine*, 16(8):10 –14, 2001.

[6] C.-H. Hsu. A newly developed infant remote monitoring system. *Journal of Medical Devices*, 2(4), 2008.

[7] M. U. Lee-Chiong TL Jr. Monitoring respiration during sleep. *Respir Care Clin N Am.*, 11(4):663–678, 2005.

[8] K. Nakajim, Y. Matsumoto, and T. Tamura. Development of real-time image sequence analysis for evaluating posture change and respiratory rate of a subject in bed. *Physiol Meas*, 22(3):N21–8, 2001.

[9] M.-Z. Poh, D. J. McDuff, and R. W. Picard. Non-contact, automated cardiac pulse measurements using video imaging and blind source separation. *Opt. Express*, 18(10):10762–10774, 2010.

[10] S. Roweis. Em algorithms for pca and spca. *in Advances in Neural Information Processing Systems*, pages 626–632, 1998.

[11] S. R. Ryu, I. Noda, and Y. M. Jung. Moving window principal component analysis for detecting positional fluctuation of spectral changes. *Bull. of the Korean Chemical Society*, 32(7):2232–2338, 2011.

[12] L. Scalise, I. Ercoli, P. Marchionni, and E. Tomasini. Measurement of respiration rate in preterm infants by laser doppler vibrometry. In *Medical Measurements and Applications Proceedings*, 2011.

[13] W. Segars, S. Mori, G. Chen, and B. Tsui. Modeling respiratory motion variations in the 4d ncat phantom. In *Nuclear Science*, 2007.

[14] C. Takano and Y. Ohta. Heart rate measurement based on a time-lapse image. *Medical Engineering and Physics*, 29(8):853–857, 2007.

[15] K. Tan, R. Saatchi, et al. Real-time vision based respiration monitoring system. In *Communication Systems Networks and Digital Signal Processing*, 2010.

[16] Z. Zhu, J. Fei, and I. Pavlidis. Tracking human breath in infrared imaging. In *Bioinformatics and Bioengineering*, 2005.